

Kinetic and interaction components of the exact time-dependent correlation potential

Kai Luo,¹ Johanna I. Fuks,¹ Ernesto D. Sandoval,¹ Peter Elliott,² and Neepta T. Maitra^{1,*}

¹*Department of Physics and Astronomy, Hunter College and the Graduate Center of the City University of New York, 695 Park Avenue, New York, New York 10065, USA*
²*Max-Planck-Institut für Mikrostrukturphysik, Weinberg 2, 06120 Halle (Saale), Germany*

(Dated: February 27, 2022)

The exact exchange-correlation (xc) potential of time-dependent density functional theory has been shown to have striking features. For example, step and peak features are generically found when the system is far from its ground-state, and these depend nonlocally on the density in space and time. We analyze the xc potential by decomposing it into kinetic and interaction components and comparing each with their exact-adiabatic counterparts, for a range of dynamical situations in model one-dimensional two-electron systems. We find that often, but not always, the kinetic contribution is largely responsible for these features, that are missed by the adiabatic approximation. The adiabatic approximation often makes a smaller error for the interaction component, which we write in two parts, one being the Coulomb potential due to the time-dependent xc hole. Non-adiabatic features of the kinetic component were also larger than those of the interaction component in cases that we studied when there is negligible step structure. In ground-state situations, step and peak structures arise in cases of static correlation, when more than one determinant is essential to describe the interacting state. We investigate the time-dependent natural orbital occupation numbers and find the corresponding relation between these and the dynamical step is more complex than for the ground-state case.

I. INTRODUCTION

Despite significant success in obtaining excitation spectra and response of molecules and solids, the reliability of time-dependent density functional theory (TDDFT) [1–3] for dynamics beyond the perturbative regime remains somewhat cloudy. TDDFT is today increasingly stepping into the fascinating playground of time-resolved dynamics in the presence of external fields, and has already proven to have made useful predictions for a number of phenomena, e.g. coherent phonon generation [4], photovoltaic design [5, 6], dynamics of molecules in strong laser fields [7], including coupling to ions [8], and attosecond control [9]. For many of these applications, there is no other practical theoretical method available that captures correlated electron dynamics for systems of these sizes. Although in theory exact, the reliability of TDDFT in practise depends on the accuracy of the available approximations for the exchange-correlation (xc) functional. Comparison with experiment, when it can be done meaningfully, shows that TDDFT often gets in the ballpark but, not always, and that there is a need to understand where the errors are in the approximations, and to develop improved approximations.

The key player in real-time TDDFT calculations is the xc potential, $v_{xc}[n; \Psi_0, \Phi_0](\mathbf{r}, t)$, a functional of the time-dependent one-body density $n(\mathbf{r}, t' < t)$, the initial interacting state Ψ_0 , and the initial Kohn-Sham (KS) state Φ_0 . Almost all calculations today use an adiabatic approximation, which inputs the instanta-

neous density into a chosen ground-state approximation: $v_{xc}^{\text{adia}}[n; \Psi_0, \Phi_0](\mathbf{r}, t) = v_{xc}^{\text{g.s.}}[n(t)](\mathbf{r}, t)$, neglecting all memory-dependence [2]. Indeed calculations with such adiabatic approximations have propelled TDDFT forward in the linear response regime, and users generally are aware to be cautious in interpreting their results for excitations for which the adiabatic approximation is known not to work (e.g. multiple excitations, long-range charge transfer between open-shell fragments, excitonic Rydberg series in solids...) [2, 3]. In some cases hybrid functionals are used, which mix in a fraction of Hartree-Fock exchange, and, via their orbital-dependence, these capture some memory-dependence and non-local spatial-dependence, while still treating correlation adiabatically. Little is known about the performance of adiabatic functionals for non-perturbative dynamics, even for systems where the adiabatic approximation is known to perform satisfactorily within the linear response regime. Beyond the linear response realm one must consider the full time-dependent xc potential, not just perturbations of it around the ground-state. To this end, there has recently been considerable effort in finding *exact* xc potentials for non-equilibrium dynamics [10–14], with the hope that analysis and understanding of their main features would lead to understanding errors in the commonly used approximations, and eventually to the development of improved functional approximations.

About 25 years ago in *ground-state* density-functional theory, decompositions of the exact ground-state xc potential into kinetic and interaction (hole) and response components began to be considered [15–18], for the purpose of analysis of the xc potential in cases where it could be calculated exactly, or highly accurately. It was found that the component due to the Coulomb poten-

* nmaitra@hunter.cuny.edu

tial of the xc hole tends to be important in real atoms and molecules in most regions, while the kinetic and response components play more of a role in intershell and bonding regions especially for “stretched” molecules, displaying step and peak features .

In the present paper we perform a similar decomposition for the time-dependent xc potential, particularly with a view to appraise the performance of the adiabatic approximation. We ask, can a decomposition into kinetic and interaction contributions in the time-domain provide us with insight and understanding of the time-dependent xc potential? Recent work [11, 13] has shown the prevalence of dynamical step features in the correlation potential in non-linear dynamics that require non-local dependence on the density in both space and time; these features appear far more generically than in the ground-state case, and are not associated with fractional charge prevention, ionization, or electric fields, as has been the case with steps found previously in time-dependent xc potentials. The physics of the time-dependent screening that the step feature, and accompanying peak, represent, have yet to be understood, and motivates the present study. Which terms in the decomposition of $v_{xc}(t)$ are largely responsible for their appearance? Although it has been shown that an adiabatic approximation completely misses the dynamical step feature – even in an *adiabatically-exact* approximation where the exact ground-state potential is used adiabatically – are adiabatic approximations to any of the individual components in the time-dependent decomposition adequate? In the ground-state, the step structure is a signature of static correlation, and we ask whether this is true also for the dynamical step. That is, is the dynamical step an indication that the system is evolving “significantly away” from a single-Slater determinant (SSD)? To this end, we investigate the dynamics of the time-dependent natural orbital occupation numbers (NOONs) of the interacting spin-summed density-matrix. More generally, we will use the decomposition to try to gain a better understanding of time-dependent correlation, steps or no steps. For example, when the system is in an excited state, there is large non-adiabatic correlation: is the kinetic or interaction component largely responsible for this? How do the kinetic and interaction components look in cases where the density of the N -electron system is a sum of N spatially-separated time-evolving one-electron densities?

Section II presents the decomposition of the xc potential into the kinetic and interaction contributions; the latter we break further into two terms, one of which is the Coulomb potential due to the time-dependent xc

hole. We briefly discuss a ground-state example, and define the NOONs in Section II A. In Section III we begin by introducing the systems and dynamics under investigation in this paper. We focus on two-electron systems in one-dimension (1D) for which numerically exact solutions to the dynamics are straightforward to obtain. To make the problem even simpler numerically we consider dynamical processes that involve essentially only two interacting states: at any time a projection onto eigenstates of the unperturbed interacting system is appreciable only for two states during the time-evolution. We study three cases: resonant Rabi oscillations induced by an electric field between the ground and lowest singlet excited state in a 1D model of the helium atom, field-free oscillations of a superposition state in the same system, and resonant excitation energy transfer in a 1D model of the hydrogen molecule. In each case we plot the exact kinetic and interaction components of the correlation potential, and compare with the adiabatically-exact approximation. We also compute the time-dependent NOONs for each case, and explore their connection with the dynamical step features. Finally, in Section IV, we briefly summarize.

II. DECOMPOSITION OF THE XC POTENTIAL

The ground-state decomposition of the xc potential explored in Refs. [15–18] was derived from taking functional derivatives of the kinetic and interaction contributions to the xc energy. In the time-dependent case, we instead consider equations of motion for the current-density and density of the interacting and KS systems. We have [1–3, 19–21]

$$\ddot{n}(\mathbf{r}, t) = \nabla \cdot (n \nabla v_{\text{ext}}) + i \nabla \cdot \langle \Psi(t) | [\hat{j}(\mathbf{r}), \hat{T} + \hat{W}] | \Psi(t) \rangle \quad (1)$$

for the interacting system, evolving under Hamiltonian $\hat{H} = \hat{T} + \hat{W} + \sum_i^N v_{\text{ext}}(\hat{r}_i, t)$, where \hat{T} and \hat{W} are the kinetic and electron-electron interaction operators respectively. Atomic units are used throughout this paper, $m_e = e^2 = \hbar = 1$. (We have omitted most variable-dependence on the right-hand-side to avoid notational clutter). A similar equation holds for the KS system where the KS Hamiltonian has $\hat{W} = 0$ and the external potential v_{ext} is replaced by the KS potential $v_s = v_{\text{ext}} + v_{\text{H}} + v_{\text{xc}}$, the sum of the external, Hartree, and xc terms. Since the KS system evolves with identical density to the interacting system, we equate the right-hand-sides of Eq. (1) and its KS analog, to find

$$\nabla \cdot (n \nabla v_{\text{xc}}) = \nabla \cdot \left[\frac{1}{4} (\nabla' - \nabla) (\nabla^2 - \nabla'^2) (\rho_1(\mathbf{r}', \mathbf{r}, t) - \rho_{1,s}(\mathbf{r}', \mathbf{r}, t)) |_{\mathbf{r}'=\mathbf{r}} + n(\mathbf{r}, t) \int n_{\text{xc}}(\mathbf{r}', \mathbf{r}, t) \nabla w(|\mathbf{r}' - \mathbf{r}|) d^3 r' \right], \quad (2)$$

where $\rho_1(\mathbf{r}', \mathbf{r}, t) = N \sum_{\sigma_1 \dots \sigma_N} \int d^3 r_2 \dots d^3 r_N \Psi^*(\mathbf{r}' \sigma_1, \mathbf{r}_2 \sigma_2 \dots \mathbf{r}_N \sigma_N; t) \Psi(\mathbf{r} \sigma_1, \mathbf{r}_2 \sigma_2 \dots \mathbf{r}_N \sigma_N; t)$ is the spin-summed one-body density-matrix of the true system of electrons with two-body interaction potential $w(|\mathbf{r} - \mathbf{r}'|)$, $\rho_{1,s}(\mathbf{r}', \mathbf{r}, t)$ is

the one-body density-matrix for the Kohn-Sham system, and $n_{xc}(\mathbf{r}', \mathbf{r}, t)$ is the xc hole, defined via the pair density, $P(\mathbf{r}', \mathbf{r}, t) = N(N-1) \sum_{\sigma_1 \dots \sigma_N} \int |\Psi(\mathbf{r}'\sigma_1, \mathbf{r}\sigma_2, \mathbf{r}_3\sigma_3 \dots \mathbf{r}_N\sigma_N; t)|^2 d^3r_3 \dots d^3r_N = n(\mathbf{r}, t) (n(\mathbf{r}', t) + n_{xc}(\mathbf{r}', \mathbf{r}, t))$.

Eq. (2) is a Sturm-Liouville equation for v_{xc} , giving a unique solution for a given density $n(\mathbf{r}, t)$ and boundary condition [20]. The first term in Eq. (2) gives a kinetic-like contribution to the xc potential while the

second term is a contribution stemming directly from the electron-electron interaction that depends on the xc hole. In 1D, Eq. (2) can be easily solved for the xc field, defined as the gradient of the xc potential:

$$\frac{d}{dx} v_{xc}(x, t) = \frac{1}{4n(x, t)} \left(\frac{d}{dx'} - \frac{d}{dx} \right) \left(\frac{d^2}{dx'^2} - \frac{d^2}{dx^2} \right) (\rho_1(x', x, t) - \rho_{1,S}(x', x, t)) \Big|_{x'=x} + \int n_{xc}(x', x, t) \frac{\partial}{\partial x} w(|x' - x|) dx'. \quad (3)$$

Note that in going from Eq. (2) to Eq. (3), we have thrown away a term of the form $g(t)/n(x, t)$, where $g(t)$ is the integration constant of the outer ∇ in Eq.(2). We do so because $g(t)$ is actually zero, due to satisfaction of boundary conditions: at the boundary of a finite system, the density decays exponentially, so to avoid the field ∇v_{xc} diverging exponentially, the integration constant $g(t)$ must be taken to be zero. We observe that, unlike in 3D where the KS and true currents may differ by a rotational component, in 1D the KS current equals the true current for finite systems, as follows from the equation of continuity. We now write $v_{xc}(x, t) = v_C^T(x, t) + v_{xc}^W(x, t)$ and define the kinetic contribution v_C^T from the first term on the right of Eq. (3):

$$v_C^T(x, t) \equiv \int^x \frac{1}{4n(x'', t)} \left(\frac{d}{dx'} - \frac{d}{dx''} \right) \left(\frac{d^2}{dx'^2} - \frac{d^2}{dx''^2} \right) (\rho_1(x', x'', t) - \rho_{1,S}(x', x'', t)) \Big|_{x'=x''} dx'', \quad (4)$$

since it arises from differences in kinetic/momentum aspects of the KS and interacting systems. Further, we denote it as a correlation contribution (hence the c subscript), since correlation generally refers to the deviation from single-Slater determinant behavior. The second term in Eq. (3) gives a contribution arising directly from the electron-interaction W , which we denote $v_{xc}^W(\mathbf{r}, t)$. We further decompose v_{xc}^W as:

$$v_{xc}^W(x, t) = v_{xc}^{\text{hole}}(x, t) + \Delta v_{xc}^W(x, t) \quad (5)$$

where v_{xc}^{hole} is the Coulomb potential of the xc hole,

$$v_{xc}^{\text{hole}}(x, t) = \int_{-\infty}^{\infty} dx' n_{xc}(x', x, t) w(|x - x'|) \quad (6)$$

while the remaining term, Δv_{xc}^W , is

$$\Delta v_{xc}^W(x, t) = - \int^x dx'' \int_{-\infty}^{\infty} dx' w(|x'' - x'|) \frac{\partial}{\partial x''} n_{xc}(x', x'', t) \quad (7)$$

where we take the lower limit of the x'' -integrations in Eq. (4) and Eq. (7) as zero in our calculations. A different choice simply shifts the potential uniformly by an irrelevant spatial constant.

Before proceeding, we consider a simple example. Consider a system of *non-interacting* electrons evolving from an initial state Ψ_0 in some potential $v(x, t)$. We may then ask whether we can find a potential in which the same non-interacting electrons evolve with exactly the same density but beginning in a different initial state Φ_0 [21, 22]. Assuming such a potential may be found,

we see that the potential that the second system evolves in is given by $v(x, t) + v_C^T(x, t)$. That is the kinetic part of the potential contains the entire difference. From this simple argument, we might expect that v_C^T in the general interacting case contains a large part of the initial-state dependent effects. In fact, in our examples that do not start from the ground-state, we shall see v_C^T is indeed the predominant term in the initial correlation potential.

Returning to the decomposition, a similar decomposition in the ground-state has led to insights for ground-state potentials in various cases [15–18, 23]. There, the exact ground-state xc potential is decomposed into a kinetic contribution v_C^{kin} , the Coulomb potential due to the xc hole v_{xc}^{hole} , and two response terms that depend on the functional derivatives of these two potentials with respect to the density, denoted together as v_{xc}^{resp} ; namely, $v_{xc}(\mathbf{r}) = v_C^{\text{kin}}(\mathbf{r}) + v_{xc}^{\text{hole}}(\mathbf{r}) + v_{xc}^{\text{resp}}(\mathbf{r})$. In real atoms and molecules at equilibrium, it is expected that v_{xc}^{hole} is the important contribution to v_{xc} in most regions, as demonstrated in Refs. [15–18]. The kinetic potential tends to give peaks in intershell regions in atoms and bonding regions in molecules, while the response potential may have step structures related to different decays of the dominant orbitals. These steps and peaks do however become more prominent in molecules stretched to large bond-lengths and are associated with static correlation. (A note if we wish to compare this decomposition with the time-dependent one presented here when applied to ground-states: although the hole potential v_{xc}^{hole} of Eq. (6) reduces to the v_{xc}^{hole} of the ground-state decomposition, v_C^T does not quite reduce to v_C^{kin} , since v_C^T

also includes part of v_C^{resp} . Likewise, Δv_C^W would then reduce to the remaining part of v_C^{resp} .)

An example of a 1D model of a LiH molecule is shown in Figure II, where two fermions, interacting via $1/\sqrt{1+(x_1-x_2)^2}$ live in the potential $v_{\text{ext}}(x) = -1/\sqrt{2.25+(x+R/2)^2} - 1/\sqrt{0.7+(x-R/2)^2}$ (see Ref [23] for details). Moving from equilibrium separation of $R = 1.6\text{au}$ to larger bond lengths, a salient feature is the build-up of the step and peak structures in v_C^T . These features are essential to prevent dissociation of the molecule into fractional charges, and to lead to the correct atomic-densities in the infinite separation limit. The kinetic component v_C^T gives the correlation potential an ultra-non-local in space character, while the hole potential, v_C^{hole} is quite local [18, 23]. In the general case, approximations in use today do a better job of capturing v_C^{hole} than of v_C^T and Δv_C^W , which require the correlation potential to have spatially non-local density-dependence.

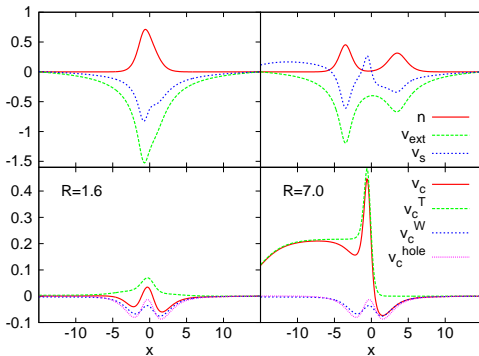


FIG. 1. Ground-state potential components for a 1D model of the LiH molecule [23] for equilibrium $R = 1.6$ a.u. (left) and stretched $R = 7.0$ a.u. (right) geometries. Top panels: density (red solid), external potential (green dashed) and Kohn-Sham potential (blue dotted). Lower panels: v_C^W (blue dotted), v_C^T (green dashed) and v_C^{hole} (pink dotted) contributions to the total correlation potential v_C (red solid).

In the present paper, we explore the decomposition represented in Eqs. (3) – (7), with the hope of gaining insight and understanding of the time-dependent xc potentials, as described in the introduction. We focus on the correlation potential here since we will consider two-electron spin-singlet systems, taking the KS state as a doubly-occupied orbital: in this case, the exchange-potential is simply minus half the Hartree-potential, $v_x(x, t) = -v_H(x, t)/2$, and the exchange-hole is minus half the density, $n_x(x, t) = -n(x, t)/2$. One focus will be on the dynamical step and peak structures found in the earlier works of Refs. [11, 13]. Quite generally, time-dependent step and peak features were

found in the time-dependent correlation potential of two-electron systems, for dynamics beyond the linear response regime [24], that cannot be captured by any adiabatic approximation. Having non-local density-dependence in space and in time, they are a challenge to incorporate in functional approximations, but their absence might have a significant effect on the dynamics. We examine the kinetic and hole contributions to the correlation potential to try to gain a better understanding of the time-dependent screening these features represent; whether the screening is largely due to kinetic or interaction effects. We already notice that such features do not appear in the hole component $v_{\text{xc}}^{\text{hole}}$: taking x large in Eq. 6 shows that asymptotically far from the system $v_{\text{xc}}^{\text{hole}} \rightarrow -1/x$, discarding the possibility of a dynamical step across the system in this component.

We will investigate whether the adiabatically-exact approximation (see Sec. III) is adequate for any of the components $v_C^T, v_C^W, v_C^{\text{hole}}$: this will indicate the “best” an adiabatic functional can do. It is not just the step structures we are interested in: we will also consider what the different components of the correlation potential and their adiabatic counterparts look like when no noticeable dynamical step is present, e.g. when the system is in an excited state (one of the time snapshots in Sec. III A), and in a case where throughout the dynamics no noticeable step features are observed (Sec. III C). In the latter case, the system consists of widely-separated atoms, each with time-evolving one-electron densities. Perhaps surprisingly, the exact correlation potential shows large features in the one-electron regions, that are completely missed by the adiabatic approximation. These features appear not only in regions of negligible density between the atoms, as has been found in the ground-state (e.g. Fig. II above), but actually in the regions where each electron lives. We show that v_C^T is responsible for these features and discuss why.

A. Natural orbitals and steps in the correlation potential

Another aspect of the dynamics we will investigate is the relation between the dynamical step structures and the time-dependent NOONs. The NOONs (defined shortly) are eigenvalues of the spin-summed one-body reduced density matrix, and take on values between 0 and 2. For a SSD, each NOON is either 2 or 0. The step structure in the *ground-state* potential indicates strong correlation in the system, with NOONs significantly away from their SSD values. For example, the largest occupation numbers in the equilibrium geometry in the model of the LiH molecule in Fig. II are 1.9551, 0.0412, 0.0035..., indicating a weakly correlated system, while for the stretched molecule at $R = 7\text{au}$ they are 1.0996, 0.8996, 0.0008... As the separation increases further, the two largest occupation numbers approach one, with all others becoming zero. This indicates a strong deviation from SSD behavior.

By diagonalizing the one-body time-dependent density-matrix of the interacting system, $\rho_1(x, x', t)$, we will investigate the connection between the time-dependent NOONs and the dynamical step. In each example, we will diagonalize the interacting ρ_1 :

$$\int \rho_1(x, x', t) \varphi_j^*(x', t) dx' = \eta_j(t) \varphi_j(x, t) \quad (8)$$

The eigenfunctions φ_j are called natural orbitals (NOs) and the eigenvalues η_j are the NOONs. In Ref. [11] it was argued that, in the two-electron case, the step structures appear at peaks of the acceleration, with magnitude given by the spatial integral of the acceleration: in the expression for the KS potential, there is a term $\int^x \partial_t(j(x', t)/n(x', t)) dx'$, where $j(x, t)$ is the one-body current-density, which is responsible for the dynamical step. It is straightforward to show that in the general N -electron case,

$$\begin{aligned} \partial_t \left(\frac{j(x, t)}{n(x, t)} \right) &= \sum_k \eta_k(t) \left(\frac{\partial_t j_k(x, t)}{n(x, t)} - \frac{j(x, t)}{n^2(x, t)} \partial_t n_k(x, t) \right) \\ &+ \sum_k \dot{\eta}_k(t) \left(\frac{j_k(x, t)}{n(x, t)} - \frac{j(x, t)}{n^2(x, t)} n_k(x, t) \right) \end{aligned} \quad (9)$$

where

$$n_k(x, t) = |\varphi_k(x, t)|^2, \text{ and} \quad (10)$$

$$j_k(x, t) = \frac{-i}{2} [\varphi_k^*(x, t) \nabla \varphi_k(x, t) - \varphi_k(x, t) \nabla \varphi_k^*(x, t)]. \quad (11)$$

The spatial integral of the right-hand-side of Eq. (9) gives the dynamical step structure studied in Ref. [11] expressed in terms of time-dependent NOs and NOONs. The relation is far from trivial, and suggests that the relation between the dynamical step and the time-dependent NOONs is not as straightforward as that between the ground-state step structures and the ground-state NOONs. We will plot the NOONs $\eta_k(t)$ for the different dynamics presented in this work, and see if any trends can be identified.

III. RESULTS: DYNAMICS OF TWO ELECTRONS IN ONE-DIMENSION

In order to find the exact xc potential Eq. (3), we must not only solve for an exact, or highly accurate, solution for the interacting wavefunction, from which we extract $\rho_1(x, x', t)$ and $n_{xc}(x, x', t)$, but we also need a method to find the exact KS density-matrix $\rho_{1,s}(x, x', t)$. In general this calls for an iterative scheme [12, 25], but for two electrons in a singlet state, assuming one starts the Kohn-Sham calculation in a single Slater-determinant, then simply requiring the doubly-occupied KS orbital

to reproduce the exact density $n(x, t)$ of the interaction problem, yields

$$\phi(x, t) = \sqrt{\frac{n(x, t)}{2}} e^{i \int^x \frac{j(x', t)}{n(x', t)} dx'} \quad (12)$$

and $\rho_{1,s}(x', x, t) = 2 \phi^*(x', t) \phi(x, t)$.

We note the alternate way of finding the correlation potential in Ref. [11]; there $v_s(x, t)$ is found first, by choosing the initial KS state to be a doubly-occupied spatial orbital and inverting the KS equations (Eq (1) of Ref. [11]). Then $v_{xc}(x, t)$ is obtained by subtracting the Hartree potential $v_H(x, t)$ and the external potential $v_{ext}(x, t)$ at time t (Eq. 2 of Ref. [11]). In the present approach, we instead extract the xc potential directly from Eq. (3). There are two advantages: the first, is that Eq. (3) is valid for N -electrons (and it's precursor Eq. (2) is valid also for three dimensions), while the expression for the KS potential used in Ref. [11] is only valid for two electrons. The second, is that since it is an expression for v_{xc} explicitly, it more readily points to what functional approximations must approximate: the right-hand-side of Eq. (3) is what needs to be approximated as a functional of the density (see also Ref. [19]). On the other hand, the expression in Ref. [11] for the xc potential has terms between the KS potential and the external potential that cancel in a subtle hidden way, and it is harder to see what terms the xc potential should be aiming to approximate.

In the following we consider various two-electron dynamics that either start in the ground-state and evolve far from it, or begin in a non-stationary state. Our 1D "electrons" interact via the soft-Coulomb interaction $w(x', x) = 1/\sqrt{(x' - x)^2 + 1}$ and live in either a 1D atom (sections III A-III B) or a 1D molecule (Section III C).

In our examples, the interacting dynamics largely, if not fully, involve two interacting states. This means that we can solve for the time-dependent interacting wavefunction $\Psi(t)$ in a particularly straightforward manner. Assuming a two-state Hilbert space,

$$|\Psi(t)\rangle = a_1(t)|\Psi_1\rangle + a_2(t)|\Psi_2\rangle, \quad (13)$$

then for the field-free cases (sections III B, III C) the time-dependent coefficients are simply given by $a_j(t) = e^{-iE_j t}$, where E_j is the eigenvalue of state Ψ_j . For dynamics in a resonant external field (section III A) the only two states involved in the dynamics are the ground state Ψ_g and the first dipole-allowed excited state Ψ_e , and $a_g(t), a_e(t)$ are solutions of the two-level Schrödinger equation,

$$i\partial_t \begin{pmatrix} a_g(t) \\ a_e(t) \end{pmatrix} = \begin{pmatrix} E_g - d_{gg}\mathcal{E}(t) & -d_{eg}\mathcal{E}(t) \\ -d_{eg}\mathcal{E}(t) & E_e - d_{ee}\mathcal{E}(t) \end{pmatrix} \begin{pmatrix} a_g(t) \\ a_e(t) \end{pmatrix} \quad (14)$$

where E_g, E_e are the energy eigenvalues of the two states, $d_{ab} = \int \Psi_a^*(x_1, x_2)(x_1 + x_2)\Psi_b(x_1, x_2)dx_1dx_2$ is the transition dipole moment and $\mathcal{E}(t) = A \cos(\omega t)$ is an applied electric field of strength A and frequency ω .

For $\omega \gg |d_{eg}A|$ and ω close to the resonant frequency, this reduces to the textbook Rabi problem; the period of the oscillations between the ground and excited state for a resonant applied field is given by $T_R = \frac{2\pi}{|d_{eg}A|}$, in the case where the ground and excited state each have a zero dipole moment, $d_{gg} = d_{ee} = 0$.

We have compared the results from the two-state approximation with a full real-space calculation, solving the exact time-dependent Schrödinger equation using the octopus code [26, 27]; aside from asymptotic features, they largely agree. We note that in the low-density region far from the system, the potential is unreliable due to noise, however this does not affect the region of interest shown in the figures. As we move out further from the atomic/molecular center, higher-excited states that are neglected in the two-state approximation come into play. These states contribute to polarization of the density, especially asymptotically where the contribution of the two lower energy states has dropped due to their faster decay. In the two-state approximation, this polarization effect is missing. When the correlation potential is extracted from the total KS potential v_s as was done in Ref. [11] a field-counteracting term appears in the correlation potential v_c to counter the external field in v_{ext} : because of the absence of polarization within the two-state model, the KS potential generated using information of the density and current-density in Ref. [11] must be flat (i.e. constant) asymptotically. However in the present approach, v_c is generated directly from Eq. (3) where the input density-matrix and xc hole are computed within the two-state approximation and so lack asymptotic polarization. This means that no field-counteracting term in the correlation potential is present in the present approach, similar to the full real-space case.

In all calculations we compare with the *adiabatically-exact* (AE) approximation: $v_c^{\text{AE}}[n; \Psi_0, \Phi_0](\mathbf{r}, t) = v_c^{\text{exact-g.s.}}[n(t)](\mathbf{r}, t)$. Note that the AE approximation for exchange coincides with the exact exchange potential for two electrons, since in this case $v_x = -v_H/2$ has only instantaneous dependence on the density. The AE approximation takes both the underlying interacting and KS wavefunctions at time t to be ground-state wavefunctions of density equal to the true density at time t . To find the AE correlation potential, we first find the ground-state interacting wavefunction of density $n(t)$, $\Psi^{\text{g.s.}}[n(t)]$, using the iterative scheme of Refs. [10, 11], and the ground-state KS wavefunction which is the doubly-occupied orbital $\sqrt{n(t)/2}$. From these, we find the reduced quantities $\rho_1^{\text{AE}}, \rho_{1,s}^{\text{AE}}$ and $n_{\text{xc}}^{\text{AE}}$ to insert into Eq. (3).

A. 1D He: Rabi dynamics to local excitations

Here we consider a 1D model of the He atom $v_{\text{ext}}(x, 0) = -2/\sqrt{x^2 + 1}$, and apply a weak resonant field $\mathcal{E}(t) = 0.00667 \cos(0.533t)$ to induce local Rabi os-

cillations between the ground and the lowest singlet excited state of the system. (The Rabi frequency is $d_{eg}A = 0.00735$ au). This system was also considered in Refs. [11, 28, 29]. Figure 2 plots the exact KS potential at four times during a half-Rabi cycle, along with the density. Step and peak structures are clearly present during the time-evolution. The step actually oscillates on the time-scale of the optical cycle, with magnitude and direction varying significantly, as evident in Figure 9, where snapshots over an optical time slice near $T_R/4$ are shown. (We comment on this figure later).

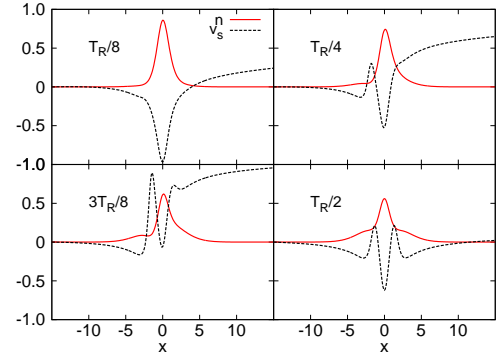


FIG. 2. (Color online) 1D He model: snapshots of density n (red solid) and exact KS potential v_s (black dashed) during a half-Rabi cycle (excited state is reached at $T_R/2$).

The correlation potential v_c is responsible for these dynamical steps, as discussed in Ref. [11], and now we investigate the role of the different components v_c^T, v_c^W , and v_c^{hole} . Figure 3 compares these components with their AE approximations, at $T_R/8$. As was noted in Ref. [11], the AE approximation does not capture the dynamical step at all, however what we find here (top right and lower left panels) is that both $v_c^{T,\text{AE}}$ and $v_c^{W,\text{AE}}$ do display a small step feature, that exactly cancel once added. Although v_c^{AE} does a poor job in approximating v_c , the AE approximation is noticeably better for the hole component: $v_c^{\text{hole,AE}}$ does somewhat capture v_c^{hole} as shown in the lower right panel, reasonably capturing the well structure. Neither the exact nor the AE v_c^{hole} component displays any step structure. These observations appeared to hold generally; for example, see Figure 4, where the components are shown at $T_R/4$. There, the step is considerably larger than at $T_R/8$, and the dominant component to the step appears in v_c^T , while at $T_R/8$, the contributions from v_c^W and v_c^T are comparable. Again, the v_c^T and v_c^W components of the AE approximation each display a (much smaller) step, but which cancel each other; again the AE approximation does a better job for v_c^{hole} than for the other components. Figure 5 shows the components at $3T_R/8$, where practi-

cally all of the step is in the kinetic component v_C^T ; still, the AE approximation approximates none of the components well.

At the time when the excited state is reached, the dynamical step wanes: as $T_R/2$ is reached, the electron dynamics slows down, and the local acceleration in the system decreases to zero (see Fig.6). As was argued in Ref. [11] the dynamical step arises from a spatial integral of the acceleration through the system, so consequently this goes to zero; the oscillations over the optical cycle become increasingly gentle and eventually vanish to zero. Figure 6 shows that still, the AE correlation potential is dramatically different from the exact potential, and that the dominant non-adiabatic features are contained in the kinetic component v_C^T . The AE approximation does not do well for any of the components, but is particularly bad for v_C^T . This can be understood from realizing that underlying the AE approximation is the assumption that both the interacting and KS states are ground-states. This is obviously not the case at half a Rabi cycle, when the true state has reached the first excited state of the system. The KS state on the other hand does have a ground-state nature (although is not the ground-state of the 1D-He potential), as it consists of a doubly-occupied node-less wavefunction. One can interpret this result in terms of initial-state dependence [22]: if we consider the states at $T_R/2$ to be initial states for subsequent dynamics, then the exact correlation potential is $v_C(T_R/2) = v_C[n, \Psi^*, \Phi^{g.s}]$ while an adiabatic approximation inherently assumes that the interacting wavefunction is a ground state instead of an excited state $v_C^{AE}(T_R/2) = v_C[n, \Psi^{g.s.}, \Phi^{g.s.}]$.

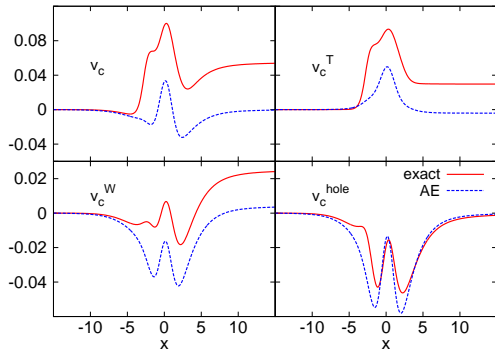


FIG. 3. (Color online) 1D He Rabi dynamics at $T_R/8$: exact (red solid) and AE (blue dashed) components of v_C as indicated.

Although the dynamical step structures look rather stark, they do tend to appear in regions where the density is small, although not negligible. A question is then, what is their impact on the dynamics? Figure 7 plots the exact dipole, compared with three TDDFT calcula-

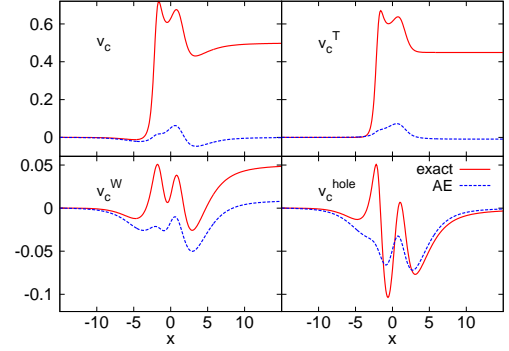


FIG. 4. (Color online) 1D He Rabi dynamics at $T_R/4$ (see caption Figure 3)

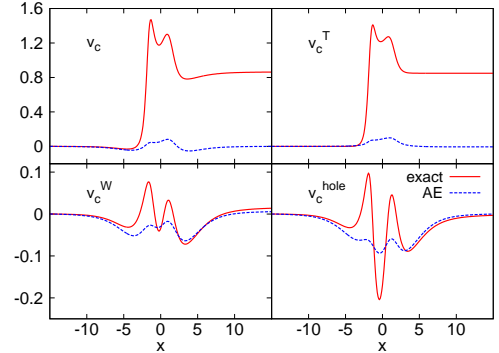


FIG. 5. (Color online) 1D He Rabi dynamics at $3T_R/8$.

tions using approximate functionals; in all calculations the same field is applied, resonant with the exact transition frequency. These approximations do quite poorly, as has also been observed in the past for Rabi dynamics [28, 29]. The linear response (LR) resonances for exact exchange (EXX), the local density approximation (LDA) and the self-interaction corrected LDA (LDA-SIC), lie at $\omega_{EXX}^{LR} = 0.549$ a.u., $\omega_{LDA-SIC}^{LR} = 0.528$ a.u. and $\omega_{LDA}^{LR} = 0.475$ a.u., whereas the exact resonance is at $\omega = 0.533$ a.u. Still, we note that recent work studying charge-transfer dynamics in the Hubbard model [30] and on 3D molecules [31] show that even when the LR frequency of the approximation is extremely close to the exact, the non-linear adiabatic dynamics can still be poor. The failure of the approximate methods is evident in Fig. 7 and is worse for the approximations with poor LR resonances. For LDA, in addition to the bad

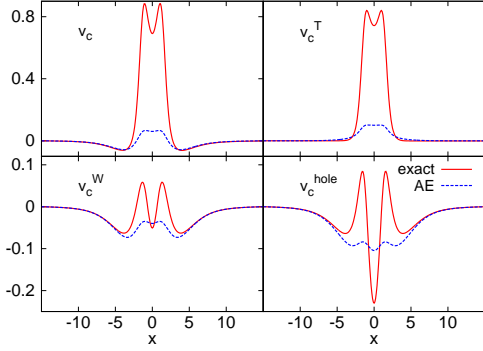


FIG. 6. (Color online) 1D He Rabi dynamics at $T_R/2$, where the true state has reached the excited state of the system.

LR frequency the ionization threshold lies already below $\omega = 0.5$ a.u., so the LDA dipole begins to probe the continuum and there is no dominant frequency. In order to assess the impact of the adiabatic approximation itself independently of the choice of the ground state approximation it would be desirable to run an AE calculation self-consistently. To this aim the iterative procedure of Ref. [10] should be performed at each time step of the propagation, which we leave to future work.

We now come to the question of the relation between the dynamical step and the NOONs. Figure 8 shows the NOONs plotted over a half-Rabi cycle: as might be anticipated, two dominate. One starts out close to 2 while the other is close to 0, and both approach 1 as the excited state is reached at $T_R/2 \approx 430$ au. In particular, we note that, in contrast with the ground-state case, there is no direct relation with the deviation from SSD and the size of the step, e.g. as we approach a half-Rabi cycle, when the interacting system is farthest from a SSD, the size of the dynamical step decreases and eventually vanishes. Instead, it seems to be related more to the local oscillatory behavior of the NOONs: Figure 9 shows the step at various times in an optical cycle near $T_R/4$ while the inset shows the corresponding NOONs. We observe that there is a correlation between the oscillations of the step and those of the NOONs. The largest(smallest) magnitude for the step size during the optical cycle appears to occur at local minima(maxima) of NOONs. This feature also holds when we zoom in to optical cycles centered around other times. Considering the complexity of Eq. (9), this result is not anticipated, and we will now turn to another example to see if the trend holds. The adiabatic NOONs (not shown), computed from diagonalizing the one-body density matrix of the interacting ground-state wavefunction of instantaneous density $n(x, t)$, have a much smaller variation. They begin at the exact values (1.9819, 0.0166, 0.0014...), make a gentle dip

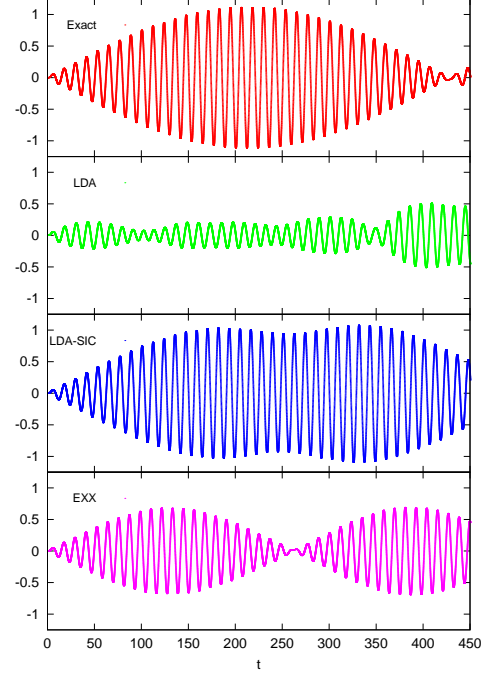


FIG. 7. (Color online) Dipole moment $d(t) = \int n(x, t)xdx$ during a half-Rabi cycle for the 1D He model. The same field is applied in all cases, $\mathcal{E}(t) = 0.00667 \cos(0.533t)$. Exact (top panel), LDA (second panel), LDA-SIC (third panel), and EXX (fourth panel).

to (1.8437, 0.0899, 0.0668...) at $T_R/2$ before rising back up: in the AE approximation the underlying ground-state remains weakly correlated throughout, as it is the ground-state of a relatively localized density.

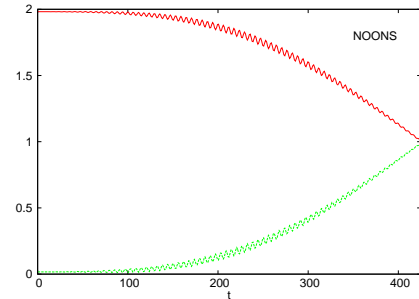


FIG. 8. (color online) The two largest time-dependent NOONs over a half-Rabi cycle for the 1D He model. All other NOONs are negligible.

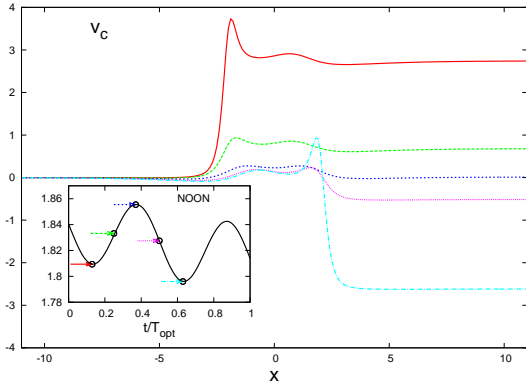


FIG. 9. (color online) 1D He Rabi dynamics: The dynamical step at snapshots over one optical cycle near $T_R/4$, i.e. at times 0.13, 0.25, 0.38, 0.5, 0.63 T_{opt} after $T_R/4$, as indicated in the inset; the coloured arrows indicate the corresponding times. The dominant time-dependent NOON is shown in the inset.

B. 1D He: Field-free evolution of a non-stationary state

In this example, we revisit the field-free evolution of a 50:50 mixture of the ground and first excited state presented in Ref. [11] in the 1D He atom,

$$|\Psi(t)\rangle = (e^{-iE_g t}|\Psi_g\rangle + e^{-iE_e t}|\Psi_e\rangle) / \sqrt{2}. \quad (15)$$

First in Figure 10, we plot the exact KS potential and the density at four times within the first half-period of the motion (the period of the dynamics is $2\pi/(E_e - E_g) = 11.788$ au). Dynamical steps are once again clearly evident, and particularly prominent at the initial time and every half-period of the evolution. There it dominates the xc potential. Figure 11 shows the correlation potential at the initial time, as well as its components v_C^T , v_C^W , and v_C^{hole} , and the AE approximation to these terms. We notice that the step is the over-riding feature of the correlation potential at this time, and is largely contained in the kinetic component v_C^T . This is consistent with the expectation expressed in Section II, that initial-state effects are largely contained in the kinetic component of the correlation potential. The AE approximation fails miserably to capture it, but does a much better job in capturing the gentle undulations of v_C^W and even more so v_C^{hole} . The v_C^W does appear to display a small step, and is fairly captured by the AE approximation at this time. At time $t = 2\text{au}$, however (Fig. 12), although the overall step size is less, the AE approximation captures neither the step in v_C^T nor in v_C^W . The AE again does a reasonable job of capturing v_C^{hole} although not getting all its structure correct, similar to the case of the local Rabi excitation in Sec. III A.

We now turn to the question of the NOONs plotted in Figure 13 over one period of oscillation. Notice that

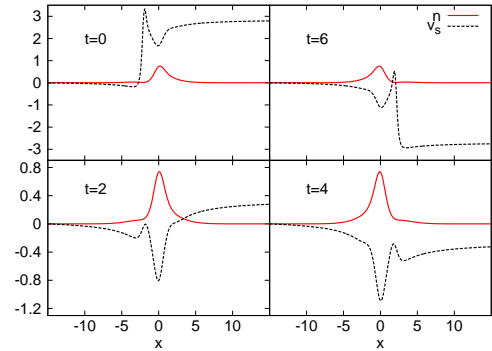


FIG. 10. The exact Kohn-Sham potential (black dashed) and density (red solid) in the field-free evolution of Eq. (15) in the 1D He at times indicated.

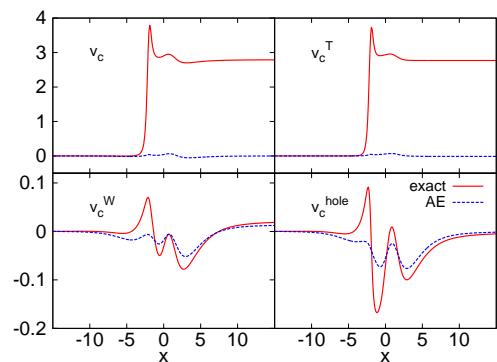


FIG. 11. (color online) Field-free evolution of Eq. (15) in 1D He: components of v_C at the initial time.

initially, the largest occupation numbers are 1.813 and 0.184, which are not very far from the SSD values of 2 and 0. Despite not deviating too far from a single-Slater determinant (i.e. being weakly correlated), the step in v_C is really quite large on the scale of the entire potential, suggesting, as in the previous section, that the system does not need to wander far from an SSD for the dynamical step to be important, in contrast to the potential steps found in the ground-state case. We note once again, that the maximum value of the step appears to appear at local minima of the NOONs (and vice-versa). Finally, Figure 14 focusses on v_C^{AE} and its components, and shows that the steps in $v_C^{W,\text{AE}}$ and $v_C^{T,\text{AE}}$ oscillate, although on a much smaller scale than the step in the exact dynamical potentials, and moreover they largely cancel when added together as noted earlier. The AE

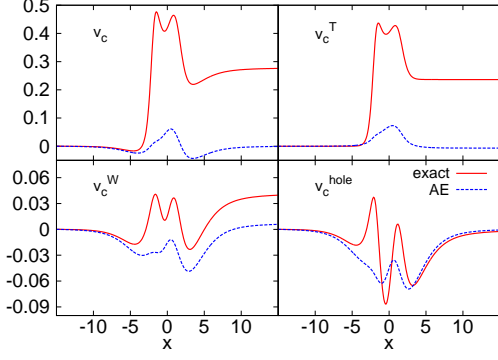


FIG. 12. (color online) As in Figure 11 but at $t = 2\text{au}$.

NOONs vary very little, and the AE system stays very weakly correlated throughout.

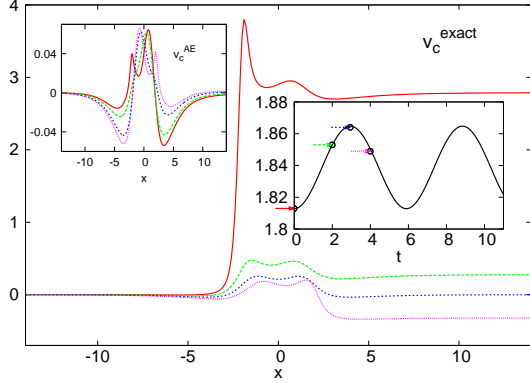


FIG. 13. The dynamical step shown at 4 times indicated in the inset, and the dominant NOON (inset) in the field-free evolution of Eq. (15) in 1D He.

C. 1D H₂: Resonant energy transfer dynamics

We now consider a case where an excitation transfers over a long distance but without charge transfer. We place our two soft-Coulomb interacting electrons in a 1D model of the H₂ molecule:

$$v_{\text{ext}}(x) = -1/\sqrt{(x - R/2)^2 + 1} - 1/\sqrt{(x + R/2)^2 + 1} \quad (16)$$

and take $R = 16$ a.u. The exact ground-state of this molecule has a Heitler-London nature in the limit of

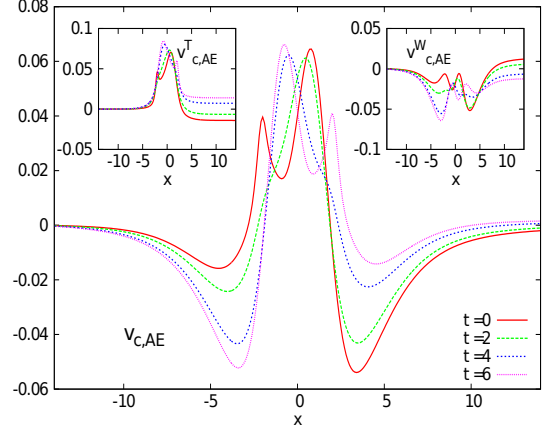


FIG. 14. The AE correlation potential, v_C^{AE} , and its components $v_C^{W,\text{AE}}$ and $v_C^{T,\text{AE}}$, in field-free evolution example. The largest adiabatic NOON is 1.94251, 1.94245, 1.94253, 1.94252 at times 0,2,4,6, respectively.

large separation,

$$\Psi^{\text{g.s.}}(x, x') = (\phi_L(x)\phi_R(x') + \phi_R(x)\phi_L(x'))/\sqrt{2} \quad (17)$$

while the lowest two singlet excitations become:

$$\begin{aligned} \Psi^{(1)}(x, x') &= (\phi_L(x)\phi_R^*(x') + \phi_L^*(x)\phi_R(x') + (x \leftrightarrow x'))/\sqrt{2} \\ \Psi^{(2)}(x, x') &= (\phi_L(x)\phi_R^*(x') - \phi_L^*(x)\phi_R(x') + (x \leftrightarrow x'))/\sqrt{2} \end{aligned} \quad (18)$$

where $\phi_{L,R}$ denote the ground-state hydrogen orbitals on the left and right atoms, and $\phi_{L,R}^*$ denote the excited state atomic orbitals. The charge-transfer resonances, $\text{H}^+\text{H}^- + \text{H}^-\text{H}^+$ (in the large separation limit), are found at higher energies in this model. We begin with an initial excitation localized in the right-hand-well, which is specifically a 50:50 combination of the first two excited states, $\Psi(0) = (\Psi^{(1)} + \Psi^{(2)})/\sqrt{2}$. The density is essentially that of a local excitation on the right atom and the ground-state on the left and is compared with the hydrogen atom ground and first excited state densities on each atom in Figure 15. The electrons are then allowed to evolve, as in the previous section, with no external field applied.

As the right-hand well de-excites, the density in the left-hand-well gets excited; the excitation transfers back and forth while the density remains integrated to one electron on each well at all times. The density and full KS potential are plotted in Figure 16 at two times during the energy transfer; T is the period of the dynamics, $T = 2\pi/(E^{(2)} - E^{(1)}) = 5374.84\text{a.u.}$ After $T/2$ the excitation has transferred completely to the other atom and the pictures at times between $T/4$ and $T/2$ are the same as those between 0 and $T/4$ but flipped around the x -axis.

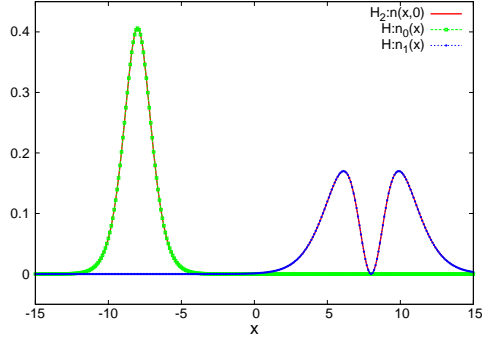


FIG. 15. Initial density in the 1D H_2 molecule $n(x, 0)$ (red solid line), compared with the ground-state density of a hydrogen atom on the left $n_0(x)$ (green points) and the excited state density of a hydrogen atom on the right $n_1(x)$ (blue points).

Any dynamical step is too small to be observed. The system seems to be essentially two one-electron systems in each well, each getting excited then de-excited; so one might expect that Hartree-xc effects are minimal, at least locally in each well and that the KS potential would revert to the external potential in the one-electron regions around each well. (Certainly, for a time-dependent truly one-electron system, $v_s = v_{\text{ext}}, v_c = 0, v_x = -v_H$). Turning to the lower panels in Figure 16 we see this is not in fact the case for the exact $v_H + v_{\text{xc}}$. The AE $v_H + v_{\text{xc}}$ does show the above described behavior, i.e. it becomes flat in the region in each well in the large separation limit and only the intermolecular midpoint peak remains. This midpoint peak is similar to the peak in the ground-state potential in H_2 that appears as the ground-state molecule dissociates [23, 32] and is a feature of the kinetic component to the correlation potential, v_c^T (see shortly). However the *exact* $v_H + v_{\text{xc}}$ is certainly nowhere near becoming flat locally around each well! The interacting system cannot be thought of as solving a one-electron Schrödinger equation in each well: although locally the density is a one-electron density, the system cannot be described by one orbital in each well.

To see this more precisely, take a look at the NOONs plotted in Figure 17 and the NOs themselves, plotted in Fig. 18. At the initial time and every half-period, there are two NOs that are equally occupied: in fact these have a bonding and antibonding structure across the molecule, and are identical up to a sign locally in each well, as can be seen from the top left panel of Fig 18. At these times therefore one orbital describes the dynamics in each well, and the problem resembles the stretched H_2 molecule (Heitler-London). In fact at $t = 0, T/2$ the exact $v_H + v_{\text{xc}}$ does become flat locally in the region of each atom (not shown). Away from the initial time and half-periods, more than two natural orbitals are significantly occupied. At a quarter-

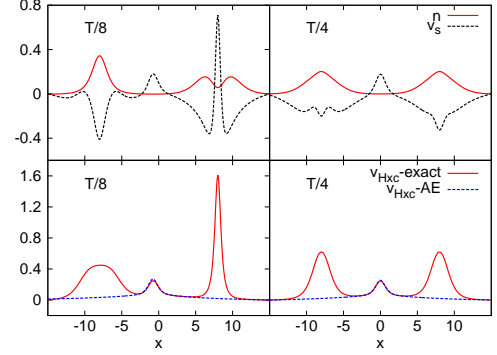


FIG. 16. Top panels: exact KS potential (black dashed) and density (red solid) at times shown during the resonant energy transfer in the H_2 molecule. Lower panels: The exact Hartree-xc potential, $v_H + v_{\text{xc}}$ (red solid) and its AE approximation (blue dashed).

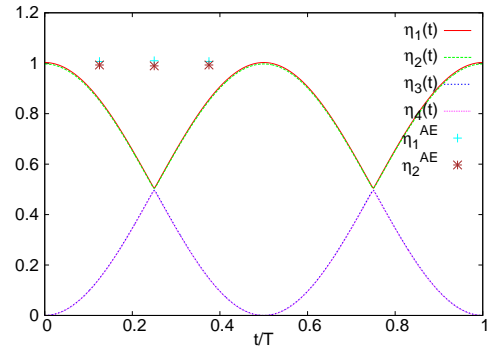


FIG. 17. The four significant NOONs over a period of oscillation of the energy transfer. The largest two AE NOONs are also shown at discrete times as points.

period, when there is equal excitation on both wells, four natural orbitals are equally occupied and these are shown on the right panels of Fig. 18. Around each well, two of the four largest natural orbitals have essentially identical densities; pairwise, they have the structure of $f_1(x) \pm f_2(x)$ where $f_{(1,2)}(x)$ is a function localized on the left(right), but, importantly, different pairs have different $f_i(x)$. This means that the electron localized in one well is being described by four orbitals, which are pairwise essentially identical, but quite distinct from the other pair. That is, each electron is locally described by two distinct functions with comparable weights: definitely not a one-electron dynamics, despite being a one-electron density. As a result the exact $v_H + v_{\text{xc}}$ does not vanish locally around each well as would be the case

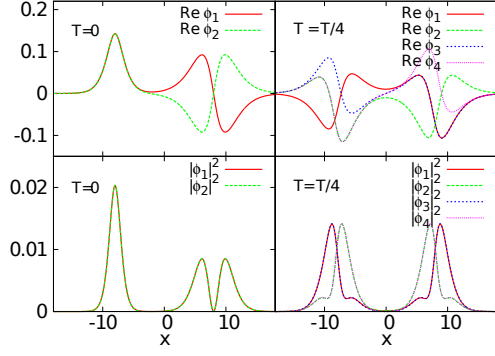


FIG. 18. (color online) Upper panel: Real part of occupied NOs at $t=0$ and $T/4$. NOs appear pairwise and have the structure $f_1(x) \pm f_2(x)$ as discussed in the text. Lower panel: orbital densities at same snapshots.

for one-electron systems (time-dependent or ground-state), see Figure 18. The excitation–de-excitation process in each well cannot be described by a pure state ($a_1\varphi_1 + a_2\varphi_2$). Note that the AE NOONs stay constant and extremely close to 1. The AE NOs (not shown) also have the symmetric/antisymmetric combination structure $g_1(x) \pm g_2(x)$, but around each well the two orbitals are essentially identical, like for the exact case at the initial time. Each electron in the AE approximation is therefore described by one function around each well, and so the system does behave locally as a one-electron system, and hence in the AE approximation the Hartree-exchange potential vanishes locally around each well.

Figures 19–20 plot the correlation potential and its components $v_c^T, v_c^W, v_c^{\text{hole}}$ at two times during the energy transfer. We observe that the AE approximation is consistently essentially exact for the interaction contributions v_c^W , and v_c^{hole} , which in fact exactly cancel the Hartree-exchange potential locally: $v_c^{W,AE} = v_c^W$ and $v_H + v_x + v_c^W = 0$ locally in each well. We can understand this, since being a one-electron density in each well, there should be no self-interaction from the Coulomb interaction, so the interaction contribution v_c^W must just cancel the Hartree and exchange potential. (Globally we have a two-electron system so $v_x = -v_H/2$ instead of completely cancelling Hartree; v_c^W then steps in to complete the job, which is called a static correlation effect and also occurs in the ground-state of stretched molecules [23, 32]). The entire non-trivial structure of v_c is in its kinetic component v_c^T , and is due to the effect discussed in the last paragraph, and is completely missed by the AE approximation, $v_c^{T,AE} = 0$ locally in each well. Similar behavior appears at other times that are not shown.

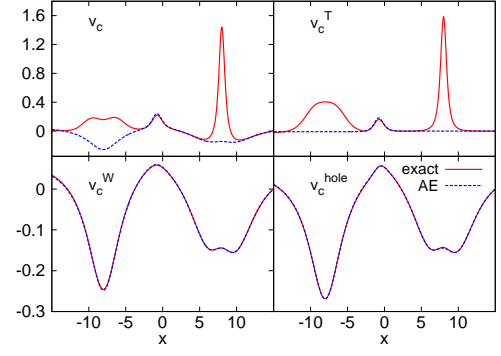


FIG. 19. (color online) Components of v_c at $t = T/8$ for the resonant energy transfer model.

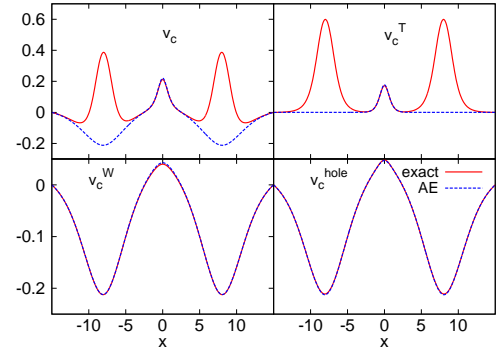


FIG. 20. (color online) Components of v_c at $t = T/4$ for the resonant energy transfer model.

IV. CONCLUSIONS AND OUTLOOK

We have presented a decomposition of the exact time-dependent xc potential into kinetic and interaction components, similar to the corresponding decomposition in the ground-state which has proven useful for understanding features of the ground-state xc potential [15–18]. We have made the first studies of these components for three different non-perturbative dynamical situations and compared them to their adiabatically-exact counterparts: resonant Rabi oscillations in a 1D He model, field-free dynamics of a superposition state in the 1D He atom, and resonant excitation energy transfer in a 1D H_2 molecule. We found that the step and peak structures in the correlation potential that were recently found in a range of dynamical situations [11, 13]

are largely, but not exclusively, contained in the kinetic component v_C^T of the correlation potential. Even in the absence of step structure, v_C^T is typically considerably worse approximated by the adiabatically-exact approximation compared to the other terms in situations far from the ground-state. The case of resonant energy transfer in the 1D H_2 molecule was an extreme case where one electron lives in each atomic well, but the excitation transferring back and forth between the atoms via the Coulomb interaction led to a large non-adiabatic component of v_C^T in each well, a signature of the fact that the dynamics in each well cannot be described by a single orbital. In this case the AE approximation for v_C^W was practically exact.

Step structures in the ground-state are associated with strong deviation from a SSD, but we found that the relationship between the time-dependent NOONs and the dynamical step is not so simple. There may be strong static correlation in the system, while there is no step, and the step may be large even when the system is weakly correlated. Instead, we found that the oscillations of the dynamical step size are associated with oscillations in the time-dependent NOONs, interestingly, and further explorations of the trends and dependences in different cases will be carried out.

The examples studied suggest that one may get away with an adiabatic approximation for v_C^{hole} , while the error from an adiabatic approximation to v_C^W and particularly v_C^T would be much larger. Still, the importance of each of these terms in influencing the dynamics has yet to be studied. A point of future study would be to self-consistently propagate separately under the three components mentioned to gauge their relative importance on the resulting dynamics. The comparison with the dipole dynamics given by adiabatic approximations (Fig. 7 for the Rabi oscillation in 1D He model, Fig. 6 of Ref. [11] for the field-free evolution in the same potential) certainly suggests that the non-adiabatic effects are important. To disentangle the effect of the adiabatic approximation itself and the choice of the ground-state approximation, a self-consistent propagation under the AE approximation would be enlightening, and is an important avenue for future work.

The equation for the exact xc potential, Eq. (3) is valid for N -electrons, and points directly to what approximations to the xc potential are attempting to model: gradients of the correlated part of the one-body density matrix (kinetic component), and Coulomb-type integrals of the xc hole (interaction components). The equation gives the xc field, i.e. the gradient of the xc potential, so even a local model of the right-hand-side could give a spatially non-local potential. The notion is somewhat reminiscent of the motivations of time-dependent current-density functional theory [33]. The step structure in the potential requires a non-local density-dependence, but the electric field it represents, ∇v_C , is quite localized.

Due to the one-body nature of the KS evolution opera-

tor, the form of the KS state at any time remains the same as that chosen for the KS initial state; orbitals composing the KS initial state evolve in time with no change in their occupations. Throughout this work, we have taken the KS initial state to be a SSD consisting of one doubly-occupied orbital. In principle, more general initial KS states may be chosen provided they have the same density and the first time-derivative of the density as that of the interacting system. The question then arises as to whether, if stuck with an adiabatic approximation, is there a choice of KS initial state that the adiabatic approximation works best for? In fact, a judicious choice of the initial KS state can lessen the error that an adiabatic approximation can make [14, 22]. For example, Ref. [22] considered the interacting system beginning in the first excited singlet state of the 1DHe atom: there the adiabatic approximation to v_{xc} initially gives a far closer approximation to the exact xc potential if the KS state is chosen as a double-Slater-determinant with one ground-state orbital and the other a lowest excited-state orbital, instead of the usual choice of a doubly-occupied orbital. This suggests to choose a KS initial state with a configuration similar to that of the true initial state to minimize the error of an adiabatic approximation at least at short times. On the other hand, when the interacting system starts in its initial ground-state, then the adiabatic approximation has least error initially if the KS initial state is also chosen as a KS ground-state: with such a choice, the adiabatically-exact approximation is exact at first. However as time evolves, the interacting state may change its form dramatically, e.g. in the example A shown in the present paper, the interacting state starts off in its ground-state, weakly-correlated, but evolves over time to an excited singlet-state that minimally requires a two-determinant description. In this case, beginning with a KS SSD, as we have done, is the best choice for the adiabatic approximation at short times, however as the excited state is reached, it becomes increasingly poor. A question for future research is whether, for a given known structure of the evolution of the interacting state, there is an optimal choice for the form of the KS wavefunction such that errors in adiabatic approximation are minimized throughout the evolution.

How significant are the structures found in the non-adiabatic parts of v_C^T and v_C^W , and their impact on the ensuing dynamics, for realistic three-dimensional systems of more than two electrons remains to be tested; this is clearly a more challenging numerical task. The analysis in terms of the kinetic and interaction contributions of the xc potential should prove useful to deepen our understanding of time-dependent electron correlation, and eventually to modelling non-adiabatic effects accurately.

Acknowledgments Financial support from the National Science Foundation CHE-1152784 (for KL), Department of Energy, Office of Basic Energy Sciences, Division of Chemical Sciences, Geosciences and Biosciences un-

der Award DE-SC0008623 (NTM., JIF), the European Communities FP7 through the CRONOS project Grant No. 280879 (PE), a grant of computer time from the CUNY High Performance Computing Center under

NSF Grants CNS-0855217 and CNS-0958379, and the RISE program at Hunter College, Grant GM060665 (ES), are gratefully acknowledged.

-
- [1] E. Runge and E.K.U. Gross, *Phys. Rev. Lett.* **52**, 997 (1984).
- [2] *Fundamentals of Time-Dependent Density Functional Theory*, (Lecture Notes in Physics 837), eds. M.A.L. Marques, N.T. Maitra, F. Nogueira, E.K.U. Gross, and A. Rubio, (Springer-Verlag, Berlin, Heidelberg, 2012); and references therein.
- [3] *Time-Dependent Density-Functional Theory: Concepts and Applications*, C. A. Ullrich, (Oxford, 2012).
- [4] Y. Shinohara et al., *J. Chem. Phys.* **137**, 22A527 (2012).
- [5] C. A. Rozzi et al., *Nature Commun.* **4** 1602 (2013)
- [6] O. V. Prezhdo, W. R. Duncan, V. V. Prezhdo, *Prog. Surf. Sci.* **84**, 30 (2009).
- [7] I. Bocharova et al., *Phys. Rev. Lett.* **107**, 063201 (2011).
- [8] S. Bubin and K. Varga, *Phys. Rev. B.* **85**, 205441 (2012).
- [9] A. Castro, *ChemPhysChem.* **14**, 1488 (2013).
- [10] M. Thiele, E.K.U. Gross, S. Kümmel, *Phys. Rev. Lett.* **100**, 153004 (2008)
- [11] P. Elliott, J. I. Fuks, A. Rubio, and N. T. Maitra, *Phys. Rev. Lett.* **109**, 266404 (2012).
- [12] J. D. Ramsden and R. W. Godby, *Phys. Rev. Lett.* **109**, 036402 (2012).
- [13] J. I. Fuks, P. Elliott, A. Rubio, and N. T. Maitra, *J. Phys. Chem. Lett.* **4**, 735 (2013).
- [14] M. Ruggenthaler, S. E. B. Nielsen, and R. van Leeuwen, *Phys. Rev. A* **88**, 022512 (2013)
- [15] M. A. Buijse, E. J. Baerends, J. G. Snijders, *Phys. Rev. A.* **40**, 4190 (1989).
- [16] O. Gritsenko, R. van Leeuwen, and E.J. Baerends, *J. Chem. Phys.* **101**, 8955 (1994)
- [17] O. Gritsenko, R. van Leeuwen, and E. J. Baerends, *J. Chem. Phys.* **104**, 8535 (1996)
- [18] O. Gritsenko and E. J. Baerends, *Phys. Rev. A.* **54**, 1957 (1996).
- [19] M. Ruggenthaler and D. Bauer, *Phys. Rev. A* **80**, 052502 (2009)
- [20] R. van Leeuwen, *Phys. Rev. Lett.* **82**, 3863 (1999).
- [21] N. T. Maitra and K. Burke, *Phys. Rev. A.* **63**, 042501 (2001).
- [22] P. Elliott, N. T. Maitra, *Phys. Rev. A* **85**, 052510 (2012).
- [23] D. J. Tempel, T. J. Martinez, N. T. Maitra, *J. Chem. Theory and Comput.* **5**, 700 (2009).
- [24] K. Luo, P. Elliott, N. T. Maitra, *Phys. Rev. A.* **88**, 042508 (2013).
- [25] M. Ruggenthaler, S. Nielsen, R. van Leeuwen, *Europhys. Lett.* **101**, 33001 (2013).
- [26] Castro, A. *et al.*. Octopus: A Tool for the Application of Time-Dependent Density Functional Theory. *Phys. Stat. Sol. (b)* **2006**, 243, 2465–2488.
- [27] Marques, M. A. L.; Castro, A.; Bertsch, G. F.; Rubio, A. Octopus: A First-Principles Tool for Excited Electron-Ion Dynamics. *Comp. Phys. Comm.* **2003**, 151, 60–78.
- [28] Fuks, J. I.; Helbig, N.; Tokatly, I.V.; Rubio, A. *Phys. Rev. B.* **2011**, 84, 075107.
- [29] M. Ruggenthaler and D. Bauer, *Phys. Rev. Lett.* **102**, 233001 (2009).
- [30] J. I. Fuks and N. T. Maitra, submitted to *Phys. Chem. Chem. Phys.* (2014).
- [31] S. Raghunathan and M. Nest, *J. Chem. Theory Comput.* **7**, 2492 (2011).
- [32] O. V. Gritsenko and E. J. Baerends, *Theor. Chem. Acc.* **96**, 44 (1997).
- [33] G. Vignale and W. Kohn, *Phys. Rev. Lett.* **77**, 2037 (1996).